Progress In Electromagnetics Research C, Vol. 135, 35–42, 2023

Quasi-Elliptic Triple Passband Filter Using Stub Loaded Step Impedance Resonator and Non-Resonating T Structure

Anirban Neogi[1, 2, *] and Jyoti R. Panda[2]

Abstract—This article presents a simple method to introduce multiple Transmission Zeros in the stopbands of a triple passband Chebyshev filter and also suppress the spurious bands below a satisfactory level, so that it can be treated as a Quasi-Elliptic filter. A pair of Stub Loaded Step Impedance Resonators (SLSIRs) is used to produce the Chebyshev filter with central passbands at 2.5, 5.5, and 9 GHz. An asymmetric Non-Resonating T (NRT) structure is implemented on each of the SLSIRs to achieve the improved skirt selectivity. Each non-resonating structure produces three Transmission Zeros (in total six). In addition to the satisfactory stopband performances, the Quasi-Elliptic triple band filter produces insertion losses of |0.4|, |0.6|, and |0.7| dB at three centre frequencies, respectively. Simulation of the proposed filter is done using HFSS13 software, and to validate the simulation, a prototype is fabricated on an Arlon AD250 (Dielectric Constant 2.5, height 0.76 mm) substrate.

1. INTRODUCTION

Good Insertion Loss (IL) and Return Loss (RL), stopband selectivity, suppression of spurious passbands are some covered research topics for multiband filters in recent past. For the sake of good stopband performances Quasi-Elliptic filters are always preferred over Chebyshev filter. Extracted pole filtering method and discriminating parallel coupling methods are some of the popular well established approaches to find the solution of controllable transmission zero (TZ) [1–5]. In a true sense, variety of methods are available to introduce TZ in Band-Pass Filter (BPF), dual or triple passband filters, or even for quad or penta band filters.

The existence of sufficient numbers of TZs in Quasi-Elliptic structure makes its stopband better than Chebyshev one. A chained-elliptic function state of art BPF [6], proximity coupling [7], or the method of parallel line coupled extended structures [8, 9] are well accepted to create TZ in the stopbands. In [10], a self coupled dual-band filter is presented, where three TZs are found between the passbands, but the spurious passbands are found above −20 dB level, which makes the skirt selectivity poorer. A Step Impedance Resonator (SIR) based dual passband filter is presented in [11] with excellent pass and stopband performances where a method of generating pole in passbands are employed, which in turn generates TZ in the stopbands. The combination of Split Ring Resonator and irregular SIR is employed in [12] to generate dual-band filter. Both the passbands are separated by TZ below −50 dB level, but the spurious passband beyond the second passband is not at all appreciable and hence degrades the stopband selectivity. The method of Non Resonating Node coupled resonators structure is used in [13], which produces TZ on both sides of multiple passbands.

In this article, we propose a miniaturised Chebyshev tri-band filter with a pair of Stub Loaded Step Impedance Resonators (SLSIRs) showing excellent passband performances (both IL and RL). For the purpose of creating TZs in the stopbands, a Non-Resonating T (NRT) structure is implemented on

Received 22 May 2023, Accepted 11 July 2023, Scheduled 21 July 2023

* Corresponding author: Anirban Neogi (anirban07.neogi@gmail.com).

[1] Supreme Knowledge Foundation Group of Institution, Hooghly 712139, West Bengal, India. [2] School of Electronics Engineering, Kalinga Institute of Industrial Technology, (Deemed to be University) Bhubaneswar 751024, Odisha, India.

both the SLSIRs. Such an NRT structure will act as an extended detuned open ended transmission line upon SLSIR. This NRT is definitely a "resonating" structure in some other frequency bands, but not in the specified stopband region. The asymmetric NRT structure has very minor effects on the passband performances but introduces multiple TZs and hence improves the stopband performance. In total, seven TZs are generated in the stopband regions, and the spurious bands in between the passbands are at least below −27 dB level. The newly designed Quasi-Elliptic triple-band filter produces ILs of |0.4|, |0.6|, and |0.7| dB at three centre frequencies 2.5, 5.5, and 9 GHz.

2. THE TRIPLE PASS BAND FILTER

As already mentioned, a pair of half wavelength ($\lambda g/2$) Stub Loaded Step Impedance Resonators (SLSIRs) is used to design the Chebyshev filter, when λg is the guided wavelength at 2.4 GHz. The basic filter design is an extended version of the design presented in [14], where by changing the admittance ratios, the dual-band filter is converted to a triple passband filter. Figure 1 depicts the basic resonator structure, its characteristics impedances, and the final triple passband filter design. The input admittance of the resonator, from the feeding point, can be divided in three parts, Y_{in1}, Y_{in2}, and Y_{in3}, as shown in Figure 1(a). Y and θ represent the characteristic admittances and electrical lengths of different sections of the resonator as shown in Figure 1(b). As per the figure, $Y_B = Y_C$, and we define the admittance ratio R as,

$$R = \frac{Y_C}{Y_A} = \frac{Y_B}{Y_A} \tag{1}$$

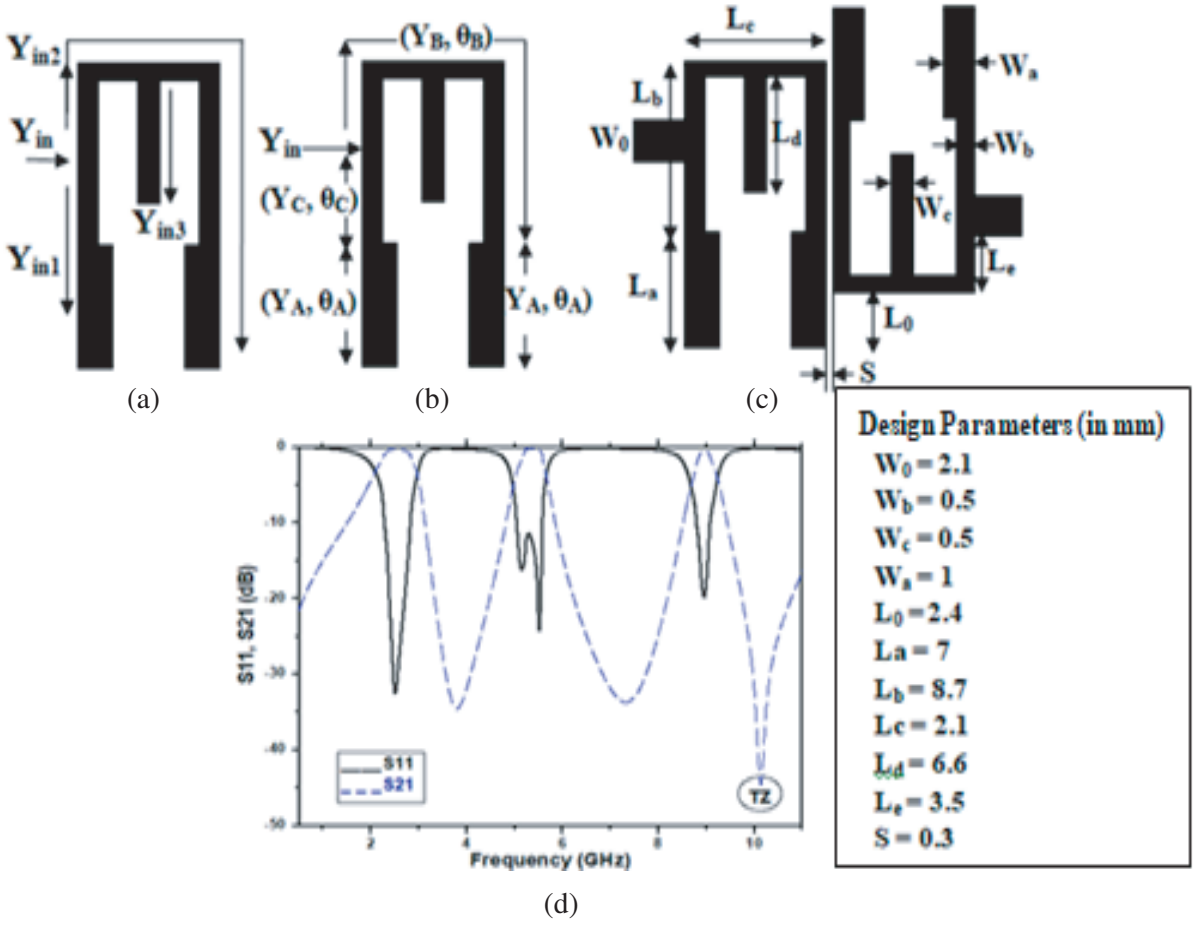

Figure 1. (a) Basic SLSIR. (b) Characteristics admittance and electrical length distribution. (c) Triple passband filter. (d) Frequency response of triple passband filter.

The admittance calculations from Figures 1(a), (b) result in Equations (2) to (5).

$$Y_{in} = Y_{in1} + Y_{in2} + Y_{in3} \tag{2}$$

$$Y_{in1} = jY_A \frac{\tan\theta_A + R\tan\theta_C}{1 - \frac{1}{R}\tan\theta_A \tan\theta_C} \tag{3}$$

$$Y_{in2} = jY_A \frac{\tan\theta_A + R\tan\theta_B}{1 - \frac{1}{R}\tan\theta_A \tan\theta_B} \tag{4}$$

$$Y_{in3} = jY_s \tan\theta_S \tag{5}$$

Putting the values of (3), (4), and (5) into Equation (2), we can deduce the resonating condition of the proposed structure [11, 14]. Clearly the structure will give us more degree of freedom and flexibility in tuning the three resonant frequencies. The frequency response of the proposed filter is shown in Figure 1(d). Three passband centre frequencies are found at 2.5, 5.5, and 9 GHz which are very much well used in wireless applications (WLAN, WiMax, and Satellite Communications, respectively). The passband |IL|s are 0.4, 0.6, and 0.7 dB, and |RL|s are found to be 33, 24, and 20 dB, respectively. Only one TZ is available at the right side of third passband at 10.1 GHz, and hence good selectivity in the stopband performance is not achieved.

3. THE QUASI-ELLIPTIC FILTER

3.1. The Non-Resonating T Structure

For the purpose of creating TZs in the stopbands, a Non-Resonating T (NRT) structure is implemented on both the SLSIRs. Such an NRT structure will act as an extended detuned open ended transmission line [15] upon SLSIR. This NRT is definitely a "resonating" structure in some other frequency bands, but not in the specified stopband region as shown in Figure 1(d), since here the two open ends of NRT are out of phase. Because of this out of phase nature NRT structures are going to contribute TZs. A symmetric NRT structure is presented in Figure 2, where Y, θ, and l represent corresponding characteristics admittances, equivalent electrical lengths, and physical lengths. From Figures 2(a) & (b), the input admittance of the symmetric NRT structure is found as

$$Y'_{in} = Y_T \frac{1 + j\frac{Y_{A'}}{Y_T}\tan\theta_{A'}}{1 + j\frac{Y_T}{Y_{A'}}\tan\theta_{A'}} \tag{6}$$

where

$$Y_T = j(Y_{B'}\tan\theta_{B'} + Y_{C'}\tan\theta_{C'}) \tag{7}$$

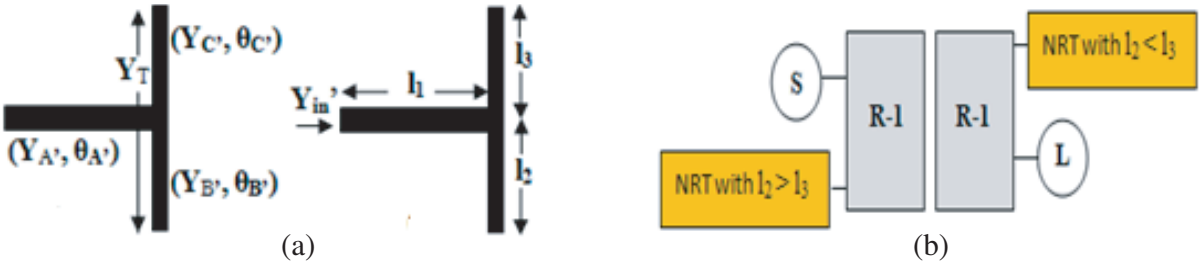

Figure 2. (a) NRT structure with admittance, electrical & physical parameters. (b) Reciprocal implementation of NRT structures on SLSIRs (R-1 & R-2).

For the NRT structure to generate TZ, $Y_{C'}$ and $Y_{B'}$ marked path must meet out of phase [16], i.e.,

$$Y_T = 0 = Y_{B'}\tan\beta_0 l_2 + Y_{C'}\tan\beta_0 l_3 = 0 \tag{8}$$

The symmetric structure (with $l_2 = l_3$), shown in Figure 2, generates a pair of attenuated poles and a pair of transmission zeros. The position of the Zeros can be controlled by changing the lengths l_2 and l_3. The position of the TZs can be approximated by experimental optimization as

$$f_{z1} = \frac{C}{2l_2\sqrt{\varepsilon_{eff}}} \tag{9a}$$

$$f_{z2} = \frac{C}{4l_2\sqrt{\varepsilon_{eff}}} \tag{9b}$$

But one very interesting fact is observed that as soon as the NRT structure is made asymmetric ($l_2 \neq l_3$), it generates three transmission zeros, i.e., it is converted into a triple mode resonator, and at three different frequencies $Y_{C'}$ and $Y_{B'}$ marked paths meet out of phase. It is worthy to mention that by adjusting the lengths of l_2 and l_3 the position of TZs can be controlled. With $l_2 > l_3$, the TZs are generated in lower frequency range, and with $l_2 < l_3$, TZs are shifted to the higher frequencies.

$$f_{z1} = \frac{l_3}{l_2}\frac{C}{2(l_2 + l_3)\sqrt{\varepsilon_{eff}}} \tag{10a}$$

$$f_{z2} = = \frac{l_3}{l_2}\frac{C}{4(l_2 + l_3)\sqrt{\varepsilon_{eff}}} \tag{10b}$$

$$f_{z3} = \frac{l_3}{l_2}\frac{C}{(2l_1 + 4l_2 + 4l_2)\sqrt{\varepsilon_{eff}}} \tag{10c}$$

Two NRT structures may be used upon two SLSIRs reciprocally (Figure 3), so that each of the three TZs can be placed in both lower and upper stop band ranges.

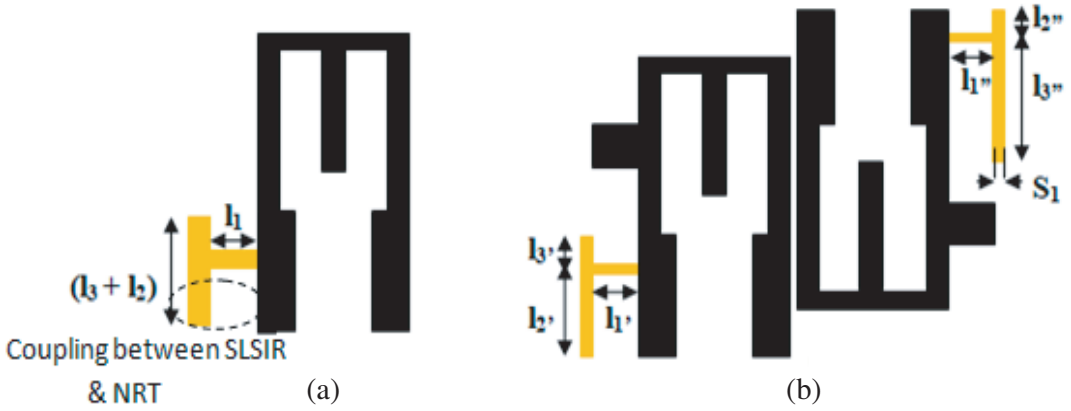

Figure 3. (a) Implementation of NRT structure as per Figure 4. (b) The final filter.

3.2. The Quasi-Elliptic Filter

Figure 3(a) shows the way the NRT structure is connected with the SLSIR. The asymmetric arrangement is shown here, where l_2 and l_3 are variables. If the SLSIR of the Figure 3(a) represents R-1, the condition $l_2 > l_3$ should be maintained, and the three TZs are generated in the lower frequency band. Similarly with SLSIR representing R-2, $l_2 < l_3$ condition is created, and three TZs are now available at high frequency band.

The final filter design is presented in Figure 3(b). Since the NRT structures are implemented over the low impedance section of SIR structure, the poles generated by the SLSIR will dominate the frequency response. Since SLSIR is not contributing any TZ in between the pass bands, the TZs generated by the NRT structures will be visible. At the input end we choose $l_{2'} > l_{3'}$, which will determine the position of three TZs in the lower stopband, specifically one at the left side and two at the right side of the first passband. Similarly at the output end $l_{2'} < l_{3'}$ condition will create one TZ

at the right side of third passband and two TZs at the left side of the same. Thus the pair of NRTs generates six TZs, so in total seven TZs are generated, and we can conclude that the Chebyshev filter is modified to Quasi-Elliptic filter. The optimized dimensions of two NRT structures are found as (in mm) $l_{1'} = 1.2$, $l_{2'} = 4.6$, $l_{3'} = 2$, $l_{1''} = 0.8$, $l_{2''} = 1$, $l_{3''} = 8.1$, and $S_1 = 0.4$.

4. THE RESULT ANALYSIS AND MEASUREMENT

When NRT-1 is implemented at the input end of SLSIR, it generates three TZs at 1.15, 3.3, and 4.2 GHz. In reverse NRT-2 implemented at output section of SLSIR generates three TZs at 7.2, 7.9, and 10.6 GHz. The comparative S_{21} graphs of NRT-1 and 2 are shown in Figure 4(a). We get the overall frequency response of the proposed filter by simultaneously implementing NRT-1 and NRT-2 structures as shown in Figure 4(b). We can achieve total seven TZs as shown in Figure 5(b). Though theoretically we assume that NRT structures are Non-Resonating, practically some couplings suffer with the SLSIR structures, especially the $(l_2 + l_3)$ section (Figure 4(a)) with the low impedance section of length L_a. Such couplings cause the TZs to be shifted slightly, which are clearly visible in Figures 5(a) and (b). Even the inherent Transmission Zero of the triple passband filter with respect to Figure 1(d) is shifted from 10.1 GHz to 9.8 GHz. In the overall response of Figure 4(b), seven TZs are found at 1.4, 3.2, 4.0, 6.8, 7.8, 9.8, and 10.4 GHz. It is well marked in the same figure that all the spurious bands are well under control. It must be mentioned that the poles contributed by the NRT structures coincide with that generated by the SLSIRs, and hence not visible in the Figure 4(b). The |IL| (0.4, 0.6 and 0.7 dB) and |RL| (25, 26 and 20 dB) at three passband frequencies are satisfactory. The passband selectivity and stopband suppression levels are well accepted as per the simulation results.

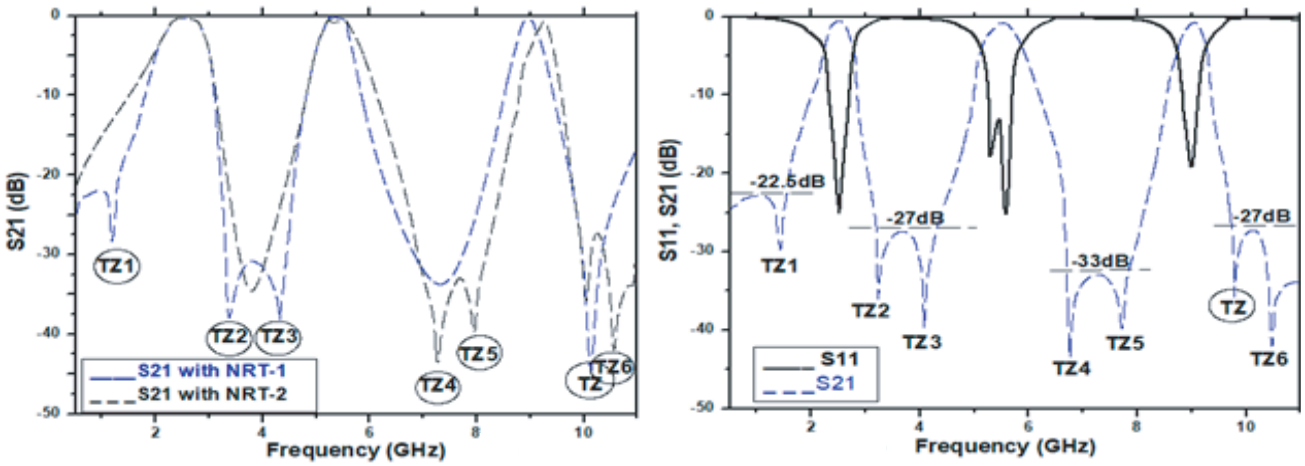

Figure 4. (a) NRT-1 & 2 implemented separately. (b) Frequency response of the proposed filter.

To validate the simulation results, a prototype of the proposed Quasi-Elliptic filter is fabricated on an Arlon AD250 substrate of dielectric constant 2.5 and height 0.76 mm. All the seven TZs are available in the measured result. Three passband centre frequencies are found at 2.53, 5.46, and 8.97 GHz with fractional bandwidth 9%, 10%, and 4%, respectively, which are almost identical to simulation results. The |IL|s at three passbands are slightly degraded to 0.6, 0.85, and 0.9 dB, respectively. The stopband suppression level is found to be excellent. The primary ambition of creating TZs in the stopbands and keeping the suppression level below an acceptable level (at least -27 dB) to improve the skirt selectivity of the filter is achieved. The fabricated prototype and the comparison of simulated and measured results are presented in Figure 5. Comparisons of the proposed filter with some other contemporary designs, which generates Quasi-Elliptic triple passband responses, are shown in Table 1.

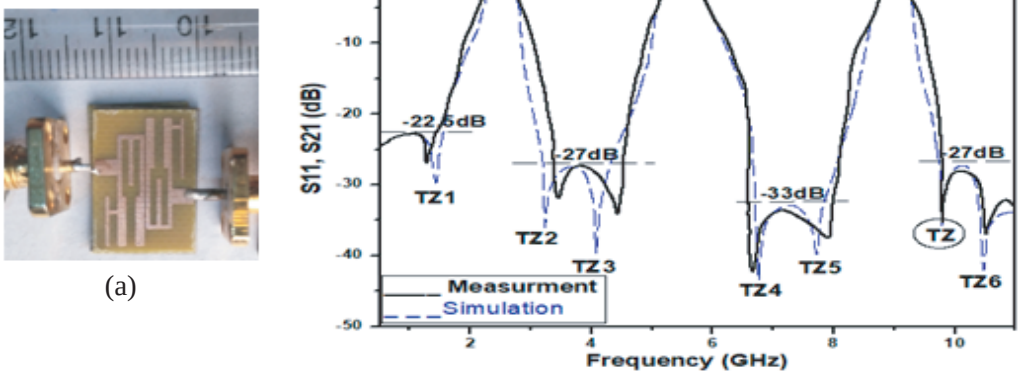

Figure 5. (a) The fabricated prototype. (b) The S_{21} comparison of simulated and measure result.

Table 1. Comparison of some contemporary designs with the proposed Quasi-elliptic filter.

Ref.	Method Used	Passband Centre Frequencies (GHz)	In-band IL(dB)	TZ before 1st and after 3rd passband	No of TZ between 1st & 2nd passband	No of TZ between 2nd & 3rd passband	Spurious bands	Size (λ_gxλ_g)
[17]	Planar HMSIW+DGS	6.28,13.19.12	1.6,0.9,0.8	Yes, Both are present	One	Two	Max. Below -25 dB	2.1x1.96
[18]	Parallel Connected Topology	1.6,1.9,2.3	1.3,2.4,1.02	Yes, Both are present	Two	Two	Max. Below -10 dB	0.1x0.23
[19]	T–inv. Cir. shaped MMR	2.4,5.91,8.86	1.6,0.73,2.8	Yes, Both are present	Two	One	Max. Below -7.5 dB	0.31x0.2
[20]	Rect. cavity Resonator	2.9,3.01,3.06	1.9, 0.5,0.7	Yes, Both are present	One	One	Max. Below -55 dB	-----
This Work	SLSIR +NRT structure	2.5,5.5,9.0	0.4,0.6,0.7	Yes, Both are present	Two	Two	Max. Below -27dB	0.13x0.16

5. CONCLUSIONS

One Quasi-Elliptic triple passband filter is introduced in this paper using SLSIR and NRT structures. The triple passband (2.5, 5.5, and 9.0 GHz) Chebyshev filtering action is generated by the SLSIR structures having poor stopband performances with only one Transmission Zero. Once the reciprocal NRT structures are implemented on SLSIRs, TZs are generated among all the passbands, and the stopband suppressions are greatly improved (at least below -27 dB). The method of NRT implementations is explained in details in the paper. The NRT structures add up six TZs (in total seven) in the frequency response of Chebyshev filter to convert it into Quasi-Elliptic filter. The overall filter performances are excellent in terms of ILs and RLs. Simulation of the proposed filter is done using HFSS13 software, and to validate the simulation, a prototype is fabricated on an Arlon AD250 (Dielectric Constant 2.5, height 0.76 mm) substrate, whose overall dimension is $(0.13\lambda_g \times 0.16\lambda_g)$. The measurement and simulation results are in great correlation with each other.

REFERENCES

1. Snyder, R. V., S. Bastioli, and G. Macchiarella, "The extracted-zero: A practical solution for transmission zeros in wideband filters," *IEEE Microwave and Wireless Components Letters*, Vol. 31, No. 9, 1043–1046, 2021.
2. Bakr, M. S., "Triple-mode microwave filters with arbitrary prescribed transmission zeros," *IEEE Access*, Vol. 9, 22045–22052, 2021.
3. Huang, Z., Y. Cheng, and Y. Zhang, "Dual-mode dielectric waveguide filters with controllable transmission zeros," *IEEE Microwave and Wireless Components Letters*, Vol. 31, No. 5, 449–452, 2021.
4. Chang, H., W. Sheng, J. Cui, and J. Lu, "Multilayer dual-band bandpass filter with multiple transmission zeros using discriminating coupling," *IEEE Microwave and Wireless Components Letters*, Vol. 30, No. 7, 645–648, 2020.
5. Guerrero, E., J. Verdú, and P. de Paco, "Synthesis of extracted pole filters with transmission zeros in both stopbands and nonresonant nodes of the same nature," *IEEE Microwave and Wireless Components Letters*, Vol. 31, No. 1, 17–20, 2021.
6. Chen, S., L.-F. Shi, G.-X. Liu, and J.-H. Xun, "An alternate circuit for narrow-bandpass elliptic microstrip filter design," *IEEE Microwave and Wireless Components Letters*, Vol. 27, No. 7, 624–626, 2017.
7. Xue, Q. and J. Y. Jin, "Bandpass filters designed by transmission zero resonator pairs with proximity coupling," *IEEE Transactions on Microwave Theory and Techniques*, Vol. 65, No. 1, 4103–4110, 2017.
8. Zhang, B., Y. Wu, and Y. Liu, "Wideband single-ended and differential bandpass filters based on terminated coupled line structures," *IEEE Transactions on Microwave Theory and Techniques*, Vol. 65, No. 3, 761–774, 2017.
9. Chen, C., "A coupled-line coupling structure for the design of quasi elliptic Bandpass filters," *IEEE Transactions on Microwave Theory and Techniques*, Vol. 66, No. 4, 1921–1925, 2018.
10. Wang, X., J. Wang, L. Zhu, W. Choi, and W. Wu, "Compact strip line dual-band bandpass filters with controllable frequency ratio and high selectivity based on self-coupled resonator," *IEEE Transactions on Microwave Theory and Techniques*, Vol. 68, No. 1, 102–110, 2020.
11. Gómez-García, R., L. Yang, J. Muñoz-Ferreras, and D. Psychogiou, "Selectivity-enhancement technique for stepped-impedance resonator dual-passband filters," *IEEE Microwave and Wireless Components Letters*, Vol. 29, No. 7, 453–455, 2019.
12. Luo, X., X. Cheng, J. Han, et al., "Compact dual-band bandpass filter using defected SRR and irregular SIR," *Electronic Letter*, Vol. 55, No. 8, 463–465, 2019.
13. Li, D., J.-A. Wang, Y. Liu, Z. Chen, and L. Yang, "Selectivity-enhancement technique for parallel-coupled SIR based dual-band bandpass filter," *Microwave and Optical Technology Letters*, Vol. 63, No. 19, 2020.
14. Gao, S., Z.-Y. Xiao, and H.-H. Hu, "A novel compact dual-band bandpass filter using SIRs with open-stub line," *China-Japan Joint Microwave Conference*, IEEE Xplore, 2008.
15. Zahedi, A., F. A. Boroumand, and H. Aliakbrian, "Analytical transmission line model for complex dielectric constant measurement of thin substrates using T-resonator method," *IET Microwaves, Antennas & Propagation*, Vol. 14, No. 15, 1919–2132, 2020.
16. Tang, J., H. Liu, and Y. Yang, "Compact wide-stopband dual-band balanced filter using an electromagnetically coupled SIR pair with controllable transmission zeros and bandwidths," *IEEE Transactions on Circuit and Systems: II*, Vol. 67, No. 11, 2357–2361, 2020.
17. Pelluri, S. and M. V. Kartikeyan, "Compact triple-band bandpass filter using multi-mode HMSIW cavity and half-mode DGS," *International Journal of Microwave and Wireless Technologies*, Vol. 13, No. 2, 103–110, 2020.
18. Cheab, S., P. W. Wong, and S. Soeung, "Design of multi-band filters using parallel connected topology," *Radioengineering*, Vol. 27, No. 1, 186–192, 2018.

19. Tripathi, S., B. Mohapatra. P. Tiwari, and V. S. Tripathi, "Multi-mode resonator based concurrent triple-band band pass filter with six transmission zeros for defence/intelligent transportation systems application," *Defence Science Journal*, Vol. 71, No. 3, 403–409, 2021.
20. Guo, Z.-C., S.-W. Wong, and L. Zhu, "Triple-passband cavity filters with high selectivity under operation of triple modes," *IEEE Transactions on Components, Packaging and Manufacturing Technology*, Vol. 9, No. 7, 1337–1344, 2019.